Delivery of Catalytic Metal Species onto Surfaces with Dendrimer Carriers for the Synthesis of Carbon Nanotubes with Narrow Diameter Distribution

ARTICLE *in* THE JOURNAL OF PHYSICAL CHEMISTRY B · NOVEMBER 2002

Impact Factor: 3.3 · DOI: 10.1021/jp026421f

4 AUTHORS, INCLUDING:

Hee Cheul Choi
Pohang University of Science and Technology
95 PUBLICATIONS **3,276** CITATIONS
SEE PROFILE

Hongjie Dai
Stanford University
382 PUBLICATIONS **80,884** CITATIONS
SEE PROFILE

THE JOURNAL OF PHYSICAL CHEMISTRY B

 VOLUME 106, NUMBER 48, DECEMBER 5, 2002

LETTERS

Delivery of Catalytic Metal Species onto Surfaces with Dendrimer Carriers for the Synthesis of Carbon Nanotubes with Narrow Diameter Distribution

Hee Cheul Choi, Woong Kim, Dunwei Wang, and Hongjie Dai*

Department of Chemistry, Stanford University, Stanford, California 94305

Received: July 1, 2002; In Final Form: September 4, 2002

Polyamidoamine (PAMAM) dendrimers are used as carriers to deliver complexed Fe(III) ions uniformly onto silicon oxide substrates for the formation of iron oxide nanoparticles with a narrow diameter in the range of 1−2 nm. Chemical vapor deposition (CVD) synthesis with these nanoparticles affords single-walled carbon nanotubes (SWNTs) with a diameter distribution in the range of 1−2 nm, much narrower than that for SWNTs grown from commonly used powder-supported catalyst (1−5 nm) and from artificial ferritin derived nanoparticles (1−3 nm). Thus, the current work represents a step further toward the synthesis of monodispersed SWNTs via the approach of chemically controlling the formation of discrete catalyst nanoparticles.

Since the first report of carbon nanotubes in 1991,[1] much effort has been taken to synthesize and elucidate the properties of these novel materials. As basic research progresses, various potential applications of carbon nanotubes have been proposed and demonstrated, such as nanoscale field effect transistor (FET),[2−4] field emission source,[5−7] sensors,[8,9] energy storage,[10,11] nanoelectrochemical electrode,[12,13] etc. Many of these applications require high quality nanotube materials in terms of purity and homogeneity in diameter and chirality. However, controlling these factors poses a significant challenge to the chemistry of nanotube synthesis. Among various synthesis methods, CVD is an approach that grows nanotubes from preformed catalytic nanoparticles, and it has been shown that the diameters of the SWNTs grown by CVD are closely determined by the diameters of catalyst particles.[14] It is therefore attractive to explore controlling the structures, e.g. diameters of SWNTs via controlling the size of catalytic seed nanoparticles, as has been pursued recently.[14−16]

Synthesis of monodispersed catalyst nanoparticles by wet chemical methods could lead to monodispersed SWNTs. However, it is difficult to achieve monodispersity for nanoparticles with diameters ∼1−2 nm that is the most typical diameter range for SWNTs. Monodispersity in this range is especially challenging for metals known to catalyze nanotube growth including Fe, Co, and Ni. In an earlier attempt, our group has shown that isolated SWNTs can be grown from preformed individual catalyst nanoparticles (iron oxide in this case) derived from artificial ferritin.[14] The empty core of an apoferritin is used as a confined space to house restricted numbers of iron species to afford artificial ferritin. One can then obtain a submonolayer of artificial ferritin on SiO_2 substrates by soaking in a ferritin solution for 30−60 min. Iron oxide nanoparticles are subsequently derived by calcination, and since the number of iron species is controlled to certain degrees inside apoferritin, the resulting iron oxide nanoparticles exhibit a diameter distribution in the range of 1−3 nm.[17] These particles are then used to synthesize SWNTs with similar diameter distribution by CVD.

Our next goal is to further narrow the size distribution of SWNTs to the 1−2 nm range. Here, we describe an approach that uses dendrimer macromolecules that have numerous reactive functional groups as hosts to complex with metal ions for the formation of catalytic nanoparticles with a narrow size distribu-

* To whom correspondence should be addressed. E-mail: hdai@stanford.edu.

10.1021/jp026421f CCC: $22.00
Published on Web 11/09/2002

SCHEME 1: A Schematic Process for Carbon Nanotube Synthesis by Chemical Vapor Deposition (CVD) on a Catalytic Nanoparticle Derived from PAMAM Dendrimer Template[a]

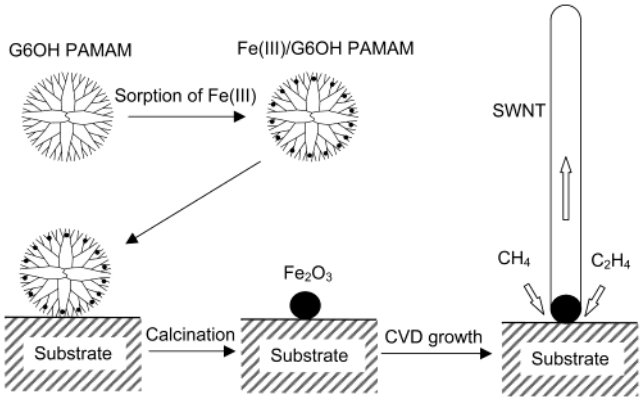

[a] Fe(III)/G6OH dendrimers are adsorbed on SiO_2 substrate followed by calcination process to remove the dendrimer and coalesce Fe(III) species into iron oxide nanoparticles. CVD growth is carried out with CH_4, H_2, and C_2H_4 at controlled flow rate (see text for details).

tion. Dendrimers are hyperbranched macromolecules well-known for various applications ranging from forming drug delivery systems,[18,19] to forming nanoparticle templates,[20−23] to forming adhesion materials for high quality metal film formation.[24,25] We show that by using dendrimers as cargos for the delivery of Fe (III) ions on to SiO_2 substrates, one can form uniform iron oxide nanoparticles on the substrates, and obtain SWNTs with diameters in the 1−2 nm range by using the nanoparticles for catalytic CVD synthesis.

Experimental Section

Our experimental procedure is shown in Scheme 1. Six-generation polyamidoamine dendrimers with 100% hydroxyl termination (15.7% in H_2O, G6OH) were purchased from Denritech, Inc. A stock solution was prepared similar to a previous work[26] by mixing 50 μL of G6OH, 100 μL of 0.1 M $FeCl_3 \cdot 6H_2O$, and 9.75 mL of double distilled water. (i.e., 1 mM $FeCl_3 \cdot 6H_2O$ with 0.0135 mM G6OH) The resulting solution provides a molar ratio between dendrimer and Fe(III) of ~1:72. The amount of Fe(III) is in excess of the maximum ion complexation capability for the 64 pairs of tertiary amines in the outmost shell of each G6OH molecule.[21] The solution was gradually mixed under continuous stirring for 30 min at room temperature. The pH of the solution was controlled (pH ~ 4) by adding hydrochloric acid, intended to avoid any possible aggregation. Right before deposition of the Fe(III) complexed dendrimers [Fe(III)/G6OH] onto a SiO_2 substrate, the stock solution was diluted 100 times (pH ~ 6.5) with double distilled water.

Si with 500 nm thick thermally grown silicon oxide (SiO_2) was used as a substrate and first cleaned by rinsing with copious amounts of isopropyl alcohol, dichloroethane, acetone, ethanol, and sulfuric acid. After several rinsing steps, the substrate was dried under a stream of Ar, and soaked into the prepared Fe(III)/G6OH solution for 5 s. The dendrimer-coated substrate was then thoroughly rinsed with double distilled water to remove any weakly bound dendrimers and dried under a stream of Ar.

Iron oxide nanoparticles were derived from the adsorbed Fe(III)/G6OH dendrimers by calcining the substrate in air at 800 °C for 5 min. CVD growth was then performed on the substrate at 900 °C for 10 min under combined flows of 1000 sccm of CH_4, 500 sccm of H_2, and 20 sccm of C_2H_4. An atomic force microscope operating in the tapping mode (AFM, Digital Instruments Nanscope III) was used to image the substrates to characterize the adsorbed dendrimers, iron oxide nanoparticles, and the synthesized SWNTs. Transmission electron microscopy (TEM) was also used to image the structures of SWNTs grown from dendrimer based nanoparticles formed on transparent SiO_2 (Ted Pella, Inc.) TEM grids. UV−vis spectroscopy (HP8453 UV−vis spectrophotometer, Agilent Tech.) was performed to monitor complexation of aqueous Fe(III) ions to tertiary amines of G6OH dendrimers. As a control experiment, we soaked SiO_2 substrates in a 1 mM $FeCl_3 \cdot 6H_2O$ aqueous solution (dendrimer-free) for various time followed by calcination and CVD growth on the substrates.

Results and Discussions

Figure 1a shows an AFM image of Fe(III)/G6OH dendrimers coated on the SiO_2 substrate. We observe that a very uniform monolayer of dendrimers is deposited on the substrate after only 5 s soaking in the 100 times diluted dendrimer solution. Previously, nanoparticles (1−2 nm in diameter) of noble metals such as Au, Pd, Pt, or Cu, and Mn have been synthesized inside dendrimer templates.[20−23,27,28] The approach involves complexation of metal ions with tertiary amine groups on the branches of the dendrimer interior followed by reduction of metal ions by BH_4^- or other types of reducing agents. In our hands, we find it difficult to obtain monodispersed Fe metal nanoparticles from Fe(III)/G6OH by the typical reduction approach due to the formation of aggregates found in the solution upon reduction reactions. Nevertheless, we find that iron oxide nanoparticles

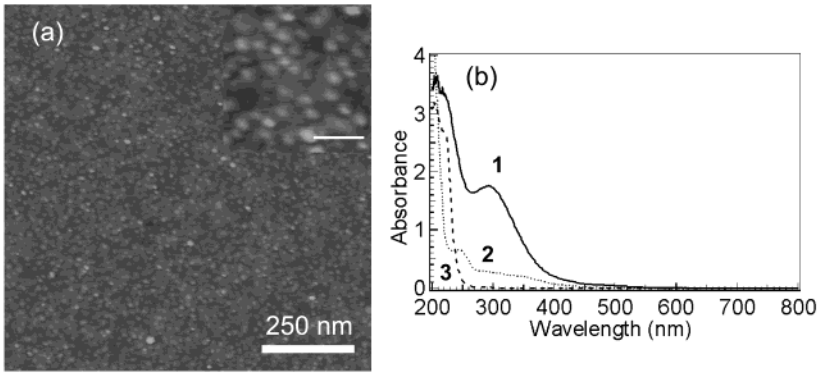

Figure 1. (a) An AFM image of Fe(III)/G6OH dendrimers adsorbed on a SiO_2 substrate. The inset in (a) shows a magnified view (scale bar: 50 nm) (b) UV−vis spectroscopy of **1**, *Fe(III) only* (solid line, 0.01 mM $FeCl_3 \cdot 6H_2O$). **2**, *Fe(III)/G6OH* (dotted line, **1** in the presence of 0.135 μM G6OH). **3**, *G6OH only* (dashed line, 0.135 μM). All solutions used here are diluted 100 times from the stock solutions. Spectrum **2** is magnified by 10 times to clarify the shifts. The optical path length was 1 cm and the temperature was 25 °C.

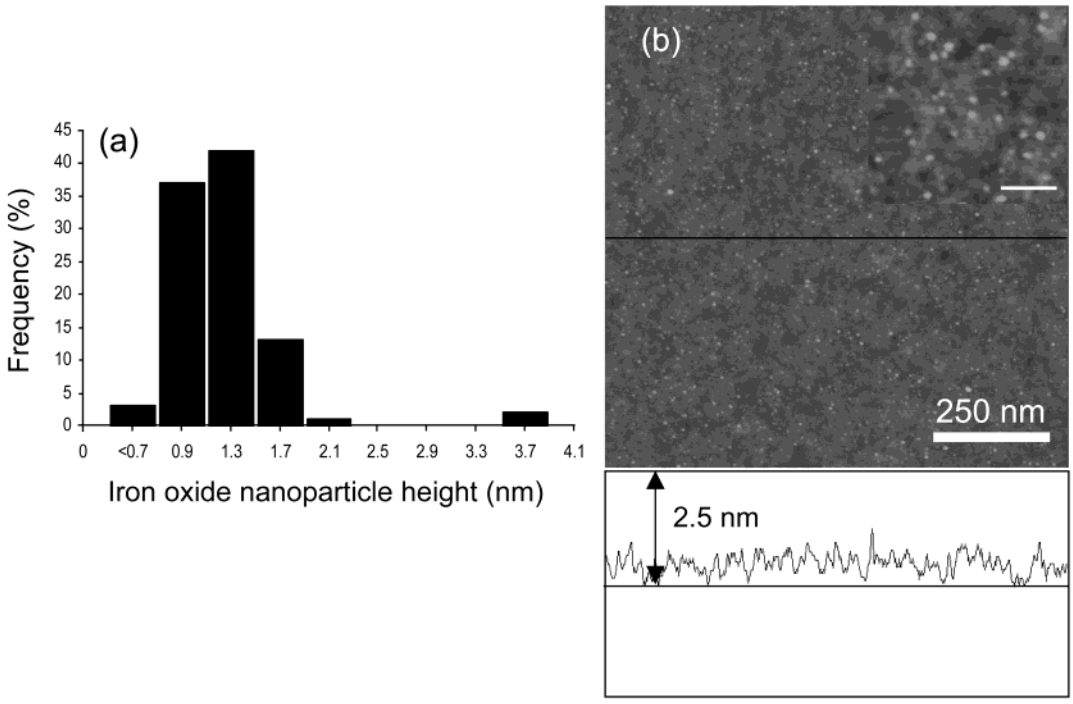

Figure 2. (a) AFM image and (b) size distribution of iron oxide nanoparticles formed after calcination of the substrate with deposited Fe(III)/G6OH dendrimers. The inset in (b) shows a magnified view (scale bar: 50 nm).

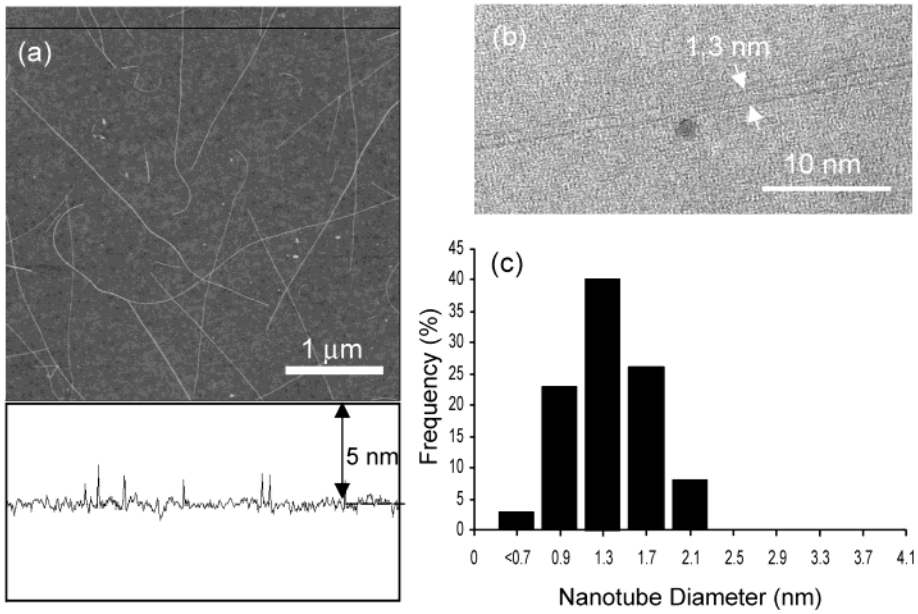

Figure 3. (a) AFM image/topographic height profile along the black line in the image, (b) TEM image, and (c) size distribution of SWNTs grown by CVD using dendrimer derived iron oxide nanoparticles.

with a narrow size distribution (Figure 2a, 1−2 nm in heights measured by AFM) are obtainable by the simple calcination/oxidation process outlined in Scheme 1. Figure 2b shows an AFM image of the discrete iron oxide nanoparticles with average diameter of 1.2 ± 0.5 nm (measured from the topographic heights of particles, root-mean-square surface roughness of SiO_2 is ∼ 0.26 nm) formed on SiO_2 surface after the calcination step. Note that the size of a 60 Fe-atom containing iron oxide nanoparticle is ∼1.4 nm.

As revealed by AFM and TEM, SWNTs are successfully grown from the iron oxide nanoparticles derived from Fe(III)/G6OH dendrimers. The growth condition which is described in the Experimental Section is identified recently by our group as a high yield condition for the synthesis of long SWNTs from discrete catalytic nanoparticles based on ferritin.[29] Figure 3a shows an AFM image of nanotubes grown under this condition. To confirm that the nanotubes are single-walled, we have carried out TEM investigations. A representative TEM image of the nanotubes is shown in Figure 3b. To facilitate TEM measurements, the substrates used for nanotube growth are commercial TEM grids coated with thin SiO_2 thin films. By so doing, we are able to perform TEM imaging of the synthesized nanotubes without any further sample preparation following CVD. The image in Figure 3b clearly shows a 1.3 nm in diameter single-walled carbon nanotube. No double- or multiwalled nanotubes have been observed with independently grown samples.

The lengths of the SWNTs are mostly in the range of 1−10 μm, while the longest nanotubes are on the order of 100 μm.

The diameters of nanotubes are measured from their topographic height with tapping mode AFM. Measurements carried out with 100 selected nanotubes show 1.4 ± 0.3 nm in diameter (Figure 3c), which is similar to that of the iron oxide nanoparticles derived from Fe(III)/G6OH. This distribution is narrower than that for SWNTs derived from ferritin (1−3 nm),[14] and significantly narrower than that for SWNTs synthesized on supported catalyst (1−5 nm).[17,30] The improved nanotube diameter distribution is a direct result of the narrow size distribution of catalytic nanoparticles derived from Fe(III)/G6OH, since the size of the particle directly determines the size of nanotube in the CVD SWNT growth process.[14] Note that we have also used TEM to survey the diameters of iron oxide nanoparticles and SWNTs. The results are very similar to those obtained by AFM measurements, since the substrates used for this work have a small roughness of ∼0.2 nm.

We now discuss the formation process for our catalytic nanoparticles. UV−vis spectrophotometric titration experiments have been performed for the solutions with various Fe(III) concentrations. The results clearly reveal that there is an obvious shift in the absorption peak due to the complexation of Fe(III) to G6OH (Figure 1b), which is attributed to the ligand−metal charge transfer (LMCT, 287 nm) effect.[31] However, unlike other transition metal ions that show drastic changes in their d−d transition absorption peaks when complexed with dendrimers,[21] no absorption peak has been observed corresponding to the d−d transition of complexed Fe(III). Quantification of the number of Fe(III) complexed with G6OH using the LMCT peaks for normalization was unsuccessful. Instead of an expected linear dependence of the LMCT peak intensity on the concentration of the Fe(III) up to a saturation point,[21] we obtained nonsystematic results, i.e., the shape and intensity of the LMCT peaks have not exhibited a clear trend upon varying the Fe(III) concentration. This indicates that the complexation of Fe(III) ions to tertiary amine groups of G6OH is not simply proportional to the concentration of the added Fe(III). In a control experiment, the pH of the Fe(III)/G6OH solution is varied by adding HCl, and it is observed that the LMCT peak is highly sensitive to the pH, but again in a nonsystematic way. Also, the pH of the Fe(III)/G6OH solution fluctuates for various concentrations of Fe(III). These results indicate that the fluctuating pH could control the effective number of protons that compete with Fe(III) for G6OH complexation. A detailed understanding of the pH effect on the complexation of Fe(III) to G6OH still requires more investigation.

The UV−vis data does qualitatively suggest strong interactions and a certain degree of complexation between Fe(III) species and G6OH dendrimers. Besides complexation with the tertiary amines in the dendrimer, it is possible that other types of interactions, e.g., hydrogen bonding interaction exists between Fe(III) species and the dendrimers. In contrast to low oxidation state complexes, such as $Zn(H_2O)_6^{2+}$ and $Cu(H_2O)_6^{2+}$, $Fe(H_2O)_6^{3+}$ tend to show very low pK_a (2.0)[31] and a strongly acidic condition is required to render this species stable. For pH > 2, reduction of the metal could occur by proton release from a water ligand as shown in eq 1.[31]

$$[(H_2O)_5Fe(OH_2)]^{3+} \leftrightarrows [(H_2O)_5Fe(OH)]^{2+} + H^+ \quad (1)$$

The Fe(II) complexes now contain hydroxide ligands, and may not undergo effective complexation with the inner tertiary amines of the dendrimers, but exhibit hydrogen bonding interactions with the exterior hydroxyl groups of G6OH.

From AFM data, we observe that the area density of iron oxide nanoparticles with appreciable diameters (> 0.7 nm) on the SiO_2 substrate is lower than that of the Fe(III)/G6OH dendrimer particles (Figure 2b vs Figure 1a). This result combined with the UV−vis data suggests that the interaction between Fe(III) and G6OH does not afford complete strong Fe(III) complexation with ∼60 Fe(III) per G6OH. The process of nanoparticle formation on the substrate then, involves release of the Fe(III) from multiple neighboring dendrimers upon calcination and the Fe(III) coalescing into 1−2 nm oxide clusters. Dendrimers containing small numbers of Fe(III) with other dendrimers in distance may result in evaporation of Fe(III) species which lead the reduced density of the particles.

The roles played by the dendrimers are 2-fold. First, the G6OH molecules act as carriers for Fe(III) species and deliver bound Fe(III) onto a SiO_2 substrate very efficiently. Investigation of the effect of soaking time finds that Fe(III)/G6OH dendrimers adsorb on SiO_2 surfaces almost instantaneously. A 1s long soaking in our dilute dendrimer solution is sufficient to form a monolayer of Fe(III)/G6OH dendrimer on the substrates (in a G6OH containing solution with 0.01 mM of $FeCl_3 \cdot 6H_2O$). In a control experiment, we soaked substrates into a comparatively high concentration of 1 mM $FeCl_3 \cdot 6H_2O$ (dendrimer-free) solution for 5s and carried out calcination. No nanotubes have been observed on the substrates after CVD growth due to negligible deposition of Fe(III) onto SiO_2. Second, the dendrimer carriers play the role of producing narrow diameter distribution of nanoparticles by delivering Fe(III) species onto SiO_2 uniformly via forming nearly homogeneous monolayers of G6OH on SiO_2 substrates.[32] This homogeneity is largely responsible for forming monodispersed nanoparticles with the Fe(III) species stored in the dendrimers. In another control experiment, we soaked a substrate in a 1 mM $FeCl_3 \cdot 6H_2O$ (dendrimer-free) solution for 10 min. The yield of nanoparticles and nanotubes obtained this way is drastically lower than those obtained by the dendrimer approach, and it exhibits wide diameter distributions in the range of 1−10 nm. Thus, deposition of Fe(III) onto SiO_2 with the pure Fe(III) solution is inhomogeneous and not controlled. With a monolayer of dendrimer carriers, Fe(III) species are delivered uniformly onto SiO_2, allowing for the formation of 1−2 nm diameter nanoparticles for CVD synthesis of SWNTs with a narrow diameter distribution.

Finally, we note that population of the nanoparticles tends to decrease after CVD process. This phenomenon is attributed to the high calcination and CVD growth temperatures. A fraction of the nanoparticles with small diameters (<1 nm) may have vaporized at these temperatures. This issue can be solved by lowering the growth temperature and is currently being investigated systematically.

Conclusion

We have demonstrated the application of PAMAM dendrimers for the synthesis of catalytic nanoparticles for the single-walled carbon nanotube growth. CVD nanotubes with a narrow diameter distribution between 1 and 2 nm are obtained from this catalyst. The initial idea of this work, i.e., forming monodispersed iron nanoparticles in dendrimer templates with one-to-one correspondence is not successful due to reasons stated above. However, we find that the G6OH dendrimers can deliver bound Fe(III) species to substrates in a highly efficient and homogeneous fashion. Calcination of the homogeneous Fe(III) containing dendrimer monolayer affords uniform catalytic particles in the 1−2 nm size range. This result hints that other organic materials can be applied to carry ion species to surfaces for catalyst applications. Homogeneous catalytic particles can

be obtained if (1) the organic materials coordinate with metal ions efficiently and (2) the organic materials containing metal ions can be deposited on the substrate in highly uniform manners. Further work along this line is being pursued for the synthesis of homogeneous single-walled carbon nanotubes and other types of catalytically grown nanowire materials.

Acknowledgment. This work is supported by the MARCO MSD Focus Center, the Packard and Sloan Foundation, a Dreyfus Teacher-Scholar Award, and a Terman Fellowship.

References and Notes

(1) Iijima, S. *Nature* **1991**, *354*, 56.
(2) Tans, S. J.; Verschueren, A. R. M.; Dekker, C. *Nature* **1998**, *393*, 49.
(3) Martel, R.; Schmidt, T.; Shea, H. R.; Hertel, T.; Avouris, P. *Appl. Phys. Lett*. **1998**, *73*, 2447.
(4) Zhou, C. W.; Kong, J.; Dai, H. J. *Appl. Phys. Lett*. **2000**, *76*, 1597.
(5) Fan, S. S.; Chapline, M. G.; Franklin, N. R.; Tombler, T. W.; Cassell, A. M.; Dai, H. J. *Science* **1999**, *283*, 512.
(6) Deheer, W. A.; Chatelain, A.; Ugarte, D. *Science* **1995**, *270*, 1179.
(7) Rinzler, A. G.; Hafner, J. H.; Nikolaev, P.; Lou, L.; Kim, S. G.; Tomanek, D.; Nordlander, P.; Colbert, D. T.; Smalley, R. E. *Science* **1995**, *269*, 1550.
(8) Shim, M.; Kam, N. W. S.; Chen, R. J.; Li, Y. M.; Dai, H. J. *Nano Lett.* **2002**, *2*, 285.
(9) Balavoine, F.; Schultz, P.; Richard, C.; Mallouh, V.; Ebbesen, T. W.; Mioskowski, C. *Angew. Chem., Int. Ed*. **1999**, *38*, 1912.
(10) Dillon, A. C.; Jones, K. M.; Bekkedahl, T. A.; Kiang, C. H.; Bethune, D. S.; Heben, M. J. *Nature* **1997**, *386*, 377.
(11) Liu, C.; Fan, Y. Y.; Liu, M.; Cong, H. T.; Cheng, H. M.; Dresselhaus, M. S. *Science* **1999**, *286*, 1127.
(12) Campbell, J. K.; Sun, L.; Crooks, R. M. *J. Am. Chem. Soc*. **1999**, *121*, 3779.
(13) Davis, J. J.; Coles, R. J.; Hill, H. A. O. *J. Electroanal. Chem*. **1997**, *440*, 279.
(14) Li, Y.; Kim, W.; Zhang, Y.; Rolandi, M.; Wang, D.; Dai, H. *J. Phys. Chem. B* **2001**, *105*, 11424.
(15) Cheung, C. L.; Kurtz, A.; Park, H.; Lieber, C. M. *J. Phys. Chem. B* **2002**, *106*, 2429.
(16) Lee, C. J.; Lyu, S. C.; Cho, Y. R.; Lee, J. H.; Cho, K. I. *Chem. Phys. Lett*. **2001**, *341*, 245.
(17) Kong, J.; Soh, H. T.; Cassell, A. M.; Quate, C. F.; Dai, H. J. *Nature* **1998**, *395*, 878.
(18) Stiriba, S. E.; Frey, H.; Haag, R. *Angew. Chem., Int. Ed*. **2002**, *41*, 1329.
(19) Esfand, R.; Tomalia, D. A. *Drug Discovery Today* **2001**, *6*, 427.
(20) Zhao, M.; Crooks, R. M. *Angew. Chem., Int. Ed. Engl.* **1999**, *38*, 364−366.
(21) Zhao, M.; Sun, L.; Crooks, R. M. *J. Am. Chem. Soc*. **1998**, *120*, 4877.
(22) Zhao, M.; Crooks, R. M. *Adv. Mater*. **1999**, *11*, 217−220.
(23) Yeung, L. K.; Crooks, R. M. *Nano Lett.* **2001**, *1*, 14−17.
(24) Rar, A.; Zhou, J. N.; Liu, W. J.; Barnard, J. A.; Bennett, A.; Street, S. C. *Appl. Surf. Sci*. **2001**, *175*−*176*, 134.
(25) Baker, L. A.; Zamborini, F. P.; Sun, L.; Crooks, R. M. *Anal. Chem*. **1999**, *71*, 4403.
(26) Niu, Y.; Yeung, L. K.; Crooks, R. M. *J. Am. Chem. Soc*. **2001**, *123*, 6840.
(27) Lemon, B. I.; Crooks, R. M. *J. Am. Chem. Soc*. **2000**, *122*, 12886.
(28) Ottaviani, M. F.; Montalti, F.; Romanelli, M.; Turro, N. J.; Tomalia, D. A. *J. Phys. Chem*. **1996**, *100*, 11033.
(29) Kim, W.; Choi, H. C.; Shim, M.; Li, Y.; Wang, D.; Dai, H. *Nano Lett.* **2002**, *2*, 703.
(30) Cassell, A. M.; Raymakers, J. A.; Kong, J.; Dai, H. J. *J. Phys. Chem. B* **1999**, *103*, 6484.
(31) Gerloch, M.; Constable, C. *Transition Metal Chemistry: The Valence Shell in d-Block Chemistry*; VCH: Weinheim, 1994.
(32) Wu, X. C.; Bittner, A. M.; Kern, K. *Langmuir* **2002**, *18*, 4984.